

Electron transport through single endohedral Ce@C₈₂ metallofullerenesSatoshi Kaneko,¹ Lu Wang,² Guangfu Luo,² Jing Lu,³ Shigeru Nagase,² Satoru Sato,⁴ Michio Yamada,⁴ Zdenek Slanina,⁴ Takeshi Akasaka,⁴ and Manabu Kiguchi¹¹*Department of Chemistry, Graduate School of Science and Engineering, Tokyo Institute of Technology, 2-12-1 W4-10 Ookayama, Meguro-ku, Tokyo 152-8551 Japan*²*Department of Theoretical and Computational Molecular Science, Institute for Molecular Science, Okazaki, Aichi 444-8585, Japan*³*State Key Laboratory of Mesoscopic Physics and Department of Physics, Peking University, Beijing 100871, P. R. China*⁴*Tsukuba Advanced Research Alliance, University of Tsukuba, Tsukuba, Ibaraki 305-8577, Japan*

(Received 15 July 2012; revised manuscript received 3 September 2012; published 5 October 2012)

The electron transport through a single endohedral Ce@C₈₂ metallofullerene bridging between metal electrodes was investigated with experimental (break junction) as well as theoretical (density functional theory coupled with the nonequilibrium Green's function formalism) techniques. The single Ce@C₈₂ molecule junction showing a high and fixed conductance value was fabricated by direct binding of the metallofullerene to Ag electrodes. The junction had a conductance of $0.28(\pm 0.05)G_0$ ($G_0 = 2e^2/h$), which was much larger than that of single molecule junctions having anchoring groups ($< 0.01G_0$), but only half that of the single C₆₀ molecule junction of $0.5G_0$. The unexpected reduced conductance of the single Ce@C₈₂ molecule junction compared with that of the single C₆₀ molecule junction was supported by the *ab initio* quantum transport calculations and was explained in terms of the localization of electrons in the C₈₂ cage. In the case of the Au electrodes, the single Ce@C₈₂ molecule junction was not formed by the break junction technique because the Ce@C₈₂ molecule could not be trapped in the large Au nanogap, which was formed just after breaking the Au contacts.

DOI: [10.1103/PhysRevB.86.155406](https://doi.org/10.1103/PhysRevB.86.155406)

PACS number(s): 73.63.Rt, 68.35.bp, 85.65.+h

I. INTRODUCTION

Developing organic electronic devices is one of the most active research fields in nanoscale science. Single-molecule electronics are one of the promising candidates in ultrasmall organic electronic devices.¹ They have a number of potential advantages, because variety of molecules enable the design of various functionalities. Based on these backgrounds, a great variety of single molecule junctions have been investigated. Currently, fabrication of a single molecule junction showing a conductance value that are both large and fixed is a prominent issue due to the fact that such a value greatly improves device performance.¹ Conventional single molecule junctions utilize anchoring groups (e.g., thiols) which chemically bind to metallic leads.²⁻⁷ These anchoring groups act as resistive spacers between the electrodes and the molecule, leading to low conductivity of the single molecule junction. Recently, highly conductive molecule junctions have been fabricated by direct binding of π -conjugated organic molecules (benzene, C₆₀) to metallic electrodes (Pt, Au, Ag) without the use of anchoring groups.⁸⁻¹² The conductive π orbital directly hybridizes with the orbital of the metal electrodes, resulting in high conductivity. Moreover, the single fullerene molecule junction preferentially shows a fixed conductance value due to its spherical molecular shape in the break junction process.^{10,12}

Among fullerene-related materials, endohedral metallofullerenes (i.e., fullerenes containing metals inside the carbon cage) have received significant attention, owing to their remarkable electrical and magnetic properties and possible applications in future molecular electronics.^{13,14} The interaction between the metal and the carbon cage play an important role in determining their unique properties, which distinguish them from their counterparts with empty carbon cages. Based on these interests as well as the unique characteristics of

single fullerene molecule junctions, electron transport through a single metallofullerene molecule has been investigated by several groups.¹⁵⁻¹⁹ Senapati *et al.* investigated the electronic structure and electron transport through a single Gd@C₈₂ molecule using theoretical calculations.¹⁵ The conductance of the single Gd@C₈₂ molecule junction was found to be smaller than that of C₈₂ due to the reduction of the transmission of the conducting channels caused by the charge localization. Yasutake *et al.* investigated electron transport through a single Tb@C₈₂ molecule on an octanethiol/Au(111) surface via scanning tunneling microscopy (STM).¹⁶ Here the switching of the single Tb@C₈₂ molecular orientation caused by the interaction between the electric dipole moment of the Tb@C₈₂ molecule and an external electric field was observed. However, electron transport through the single metallofullerene bridge between metal electrodes has never been directly measured.

In the present study we have fabricated a single metallofullerene molecule junction for the first time and investigated its electron transport properties using a mechanically controllable break junction (MCBJ) in ultrahigh vacuum (UHV). The single Ag/Ce@C₈₂/Ag molecule junction showed a high and fixed conductance value of $0.28(\pm 0.05)G_0$ ($G_0 = 2e^2/h$), which was much larger than that of single molecule junctions having anchoring groups ($< 0.01G_0$), but only half that of the single C₆₀ molecule junction of $0.5G_0$. The reduction of the conductance of the single Ce@C₈₂ molecule junction compared with that of the single C₆₀ molecule junction was explained in terms of the localization of electrons in the C₈₂ cage using the *ab initio* quantum transport calculations. In the case of the Au electrodes, the single Ce@C₈₂ molecule junction was not formed by the break junction technique because the Ce@C₈₂ molecule could not be trapped in the large Au nanogap, which was formed just after breaking the Au contacts.

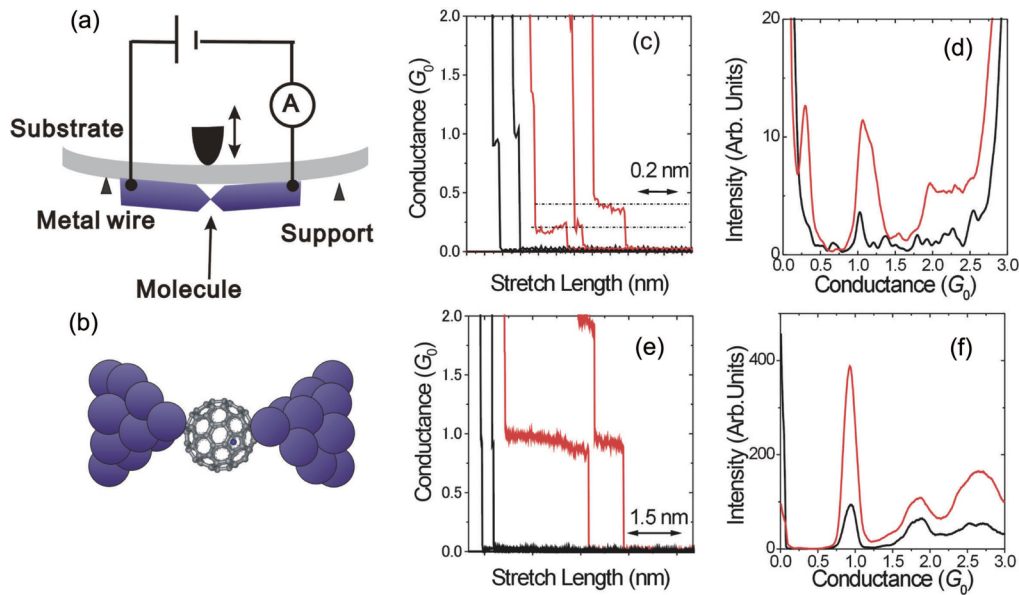


FIG. 1. (Color online) (a) Experimental setup and (b) schematic view of the single Ce@C₈₂ molecule junction. (c), (e) Typical conductance traces, and (d), (f) histograms of Ag and Au contacts after the introduction of Ce@C₈₂. The metal electrodes were (c), (d) Ag, and (e), (f) Au. The black traces and histograms indicate the values obtained for the clean Ag or Au contacts. The intensity of the conductance histograms was normalized with the number of the conductance traces. The conductance histograms were constructed without data selection from 1000 conductance traces of breaking metal contacts. The bin size was $0.004G_0$.

II. EXPERIMENT

Soot containing Ce@C₈₂ was prepared according to the reported procedure¹⁴ by the dc arc vaporization method using a composite anode, which contains graphite and cerium oxide with the atomic ratio of Ce/C equal to 2.0%. The composite rod was subjected to an arc discharge as an anode under a pressure of 150 Torr He. The raw soot was collected and extracted with 1,2,4-trichlorobenzene solvent for 15 h. The soluble fraction was injected into the HPLC; a PYE column (20 mm × 250 mm i.d.; Cosmosil, Nacalai Tesque Inc.) was used in the first step and a Buckyprep column (20 mm × 250 mm i.d.; Cosmosil, Nacalai Tesque Inc.) in the second step to give pure Ce@C₈₂.

The conductance measurements were performed in a custom-designed UHV system at 300 K equipped with a MCBJ.²⁰ Details of the experimental design have been previously reported by our group.¹² The vacuum chamber was evacuated with a turbo molecular pump (TMP: 250 l/s) or sputter-ion pump (IP: 270 l/s). Since the mechanical vibration from the TMP affected the conductance measurements of the single molecular junctions, the chamber was evacuated by only IP during the conductance measurements. The base pressure was 2×10^{-7} Pa. A notched Au or Ag wire (0.1 mm in diameter, 10 mm in length) was fixed with epoxy adhesive on top of a phosphorous bronze plate covered with a thin polymer foil. The substrate was mounted in a three-point bending configuration inside the UHV chamber. While under UHV, the wire was mechanically broken by bending the substrate, and clean surfaces were exposed. The bending could be precisely controlled using a piezo element, which enable us to form atomic contacts. 1 ML (mono layer) Ce@C₈₂ was deposited on the Au and Ag contacts with a Knudsen cell before stretching the contacts. The distance between the Knudsen cell and the sample was 200 mm. The temperature

of the sample was 300 K and the pressure was kept below 5×10^{-6} Pa during the deposition process. The amount of deposited Ce@C₈₂ was monitored with a thickness monitor. dc two-point voltage-biased conductance was measured during the breaking process under an applied bias voltage of 100 mV between the electrodes. The bias voltage was sourced by PCI-MIO-16XE-10 AD converter (National Instrument) and current was measured by Keithley 6487 picoammeter. The electric noise level was below $2 \times 10^{-3}G_0$ under an applied bias voltage of 100 mV in this setup. Typically, the metal contact was repeatedly formed and broken at 6 Hz. A single conductance trace of 2500 points were recorded in 80 ms during the breaking the contact. At least 1000 traces were recorded for each sample. Artificial selection of the specific trace was not carried out at the construction of the histogram. The experiments were performed for five distinct samples.

Figure 1(c)–1(f) show the typical conductance traces and conductance histograms during the breaking of the Au or Ag contacts before and after introduction of Ce@C₈₂. The stretch length is the displacement between the stem parts of the metal electrodes which are fixed with epoxy adhesive. Before introduction of Ce@C₈₂, immediately preceding separation of the Au and Ag electrodes, the conductance was $1G_0$ ($G_0 = 2e^2/h$, where e is the charge of an electron, and h is Planck's constant), which corresponded to Au and Ag atomic contacts.¹ The corresponding conductance histograms showed clear $1G_0$ peaks. After introduction of Ce@C₈₂ to Ag contacts, the $1G_0$ plateau was elongated in the conductance traces, and the $1G_0$ peak was enhanced in the conductance histograms. A new sequence of steps appeared in the conductance traces at the lower conductance region [Fig. 1(c)]. The conductance value of the steps was an integer multiple of 0.2–0.3 G_0 . The corresponding conductance histogram showed a peak

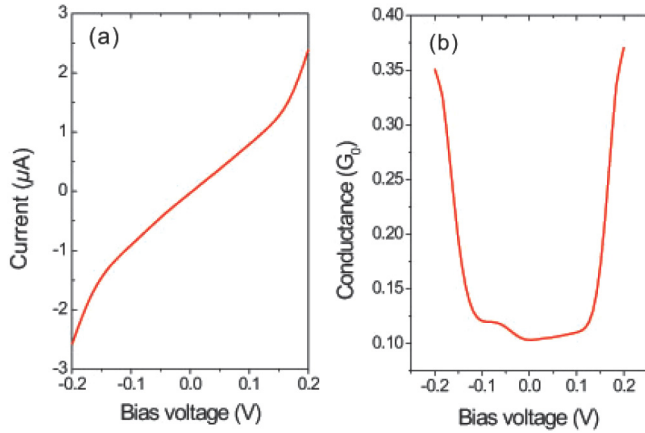


FIG. 2. (Color online) (a) I - V curve and (b) the first derivative for the single Ag/Ce@C₈₂/Ag molecule junction. The I - V curve was measured by a direct current (dc) method at 300 K.

around $0.3G_0$ [Fig. 1(d)]. There were only few steps in the conductance traces below $0.1G_0$, and features were not observed in the conductance histograms below $0.1G_0$. These experimental results suggest that the Ce@C₈₂ molecule was trapped between the Ag nanogap, and the steps in the traces and peak in the histogram showing values of 1×0.2 – $0.3G_0$ and 2×0.2 – $0.3G_0$ could be ascribed to one and two Ce@C₈₂ molecules bridging between Ag electrodes. From repeated measurements, the conductance of the single Ag/Ce@C₈₂/Ag molecule junctions was determined to be $0.28 (\pm 0.05)G_0$, which was much larger than that of single molecule junctions having anchoring groups ($<0.01G_0$).^{2–6} The appearance of the sharp peak in the conductance histogram also showed the formation of the single molecule junction with a fixed conductance value. We could fabricate a single Ce@C₈₂ molecule junction exhibiting a high and fixed conductance value via direct binding of the π -conjugated metallofullerene molecule to the Ag electrodes.

While the single Ce@C₈₂ molecule junctions were formed using Ag electrodes, they were not formed using Au electrodes. No plateaus or features were observed in the conductance traces [Fig. 1(e)] or histograms [Fig. 1(f)] below $1G_0$ for Au contacts after the introduction of Ce@C₈₂. The elongation of the $1G_0$ plateau in the conductance traces and enhancement of the $1G_0$ peak in the conductance histogram were observed, as is the case with the Ag contacts after the introduction of Ce@C₈₂.

The current-voltage (I - V) curves were measured for the single Ag/Ce@C₈₂/Ag molecule junctions by a direct current (dc) method where each curve was recorded at fixed electrodes separation at 300 K. The dc voltage was scanned from -0.2 V to $+0.2$ V (positive scan), or from $+0.2$ V to -0.2 V (negative scan) with step voltage of 0.004 V. The I - V curves showing similar curves with positive and negative scans were adopted in the present study. Figure 2 shows the I - V curve and the first derivative for the single Ag/Ce@C₈₂/Ag molecule junction, where the I - V curve were obtained by averaging the six I - V curves. Symmetric upward step in conductance was observed at ± 0.12 V. This conductance enhancement around ± 0.12 V were observed for three distinct samples. The conductance enhancement could be explained by approaching

the Fermi level of the Ag electrode to the molecular level of Ce@C₈₂ by increasing the bias voltage. Although simple comparison between the threshold energy and molecular level is not appropriate for the single molecule junction,²⁰ there is some relationship between threshold energy and energy difference in molecular orbital and Fermi level. In the case of single Au/benzenedithiol/Au molecule junction, the conductance enhancement was observed at bias voltage of 1 V.²¹ The energy difference between the Fermi level and HOMO (conduction orbital) is 1.2 eV for the Au/benzenedithiol/Au molecule junction, which agrees with the threshold voltage of 1 eV.²² Since the energy difference between the Fermi level of Ag electrode and conduction orbital of Ce@C₈₂ is much smaller than the Au/benzenedithiol/Au molecule junction due to the small energy gap, the threshold voltage decreased to low value, which might lead to appearance of the conductance enhancement at ± 0.12 V in I - V curves.

Using a similar direct binding technique, we have measured the conductance of a single C₆₀ molecule trapped in the Au and Ag nanogaps under UHV at 300 K in the previous study.¹² The conductances of the single Au/C₆₀/Au junction and Ag/C₆₀/Ag junctions were $0.3(\pm 0.1)$ and $0.5(\pm 0.1)G_0$, respectively. The Table I is the summary of the conductance for the single C₆₀ and Ce@C₈₂ molecular junctions. The conductance of the single fullerene molecule was reduced by the introduction of Ce metal, which appeared contradictory to the corresponding reduction in the HOMO-LUMO gap.¹³ In the simple tunneling model,¹ the conductance of the single molecule junction increases with the decrease in the energy difference between the Fermi level and the conduction orbital relating to the HOMO-LUMO gap. We will discuss this point in the theoretical part.

The Au/Ce@C₈₂/Au junction was not formed, whereas Au/C₆₀/Au and Ag/Ce@C₈₂/Ag junctions were formed in the present study. These experimental results can be explained by the difference in the electrode gap distance of the nanogap formed by breaking the metal electrodes. Figure 3 shows the length histogram of the $1G_0$ plateau, which corresponds to Au or Ag atomic contact.¹ Since the probability of the appearance of the $1G_0$ plateau was quite low for a clean Ag contact, we did not evaluate the length histogram for this situation. For the clean Au, Au/C₆₀/Au, and Ag/Ce@C₈₂/Ag junctions, the Au and Ag atomic contacts ($1G_0$) broke within 0.3 nm. In contrast, the Au atomic contact could be stretched up to 1.4 nm after the introduction of Ce@C₈₂. Most of junction stretched more than 0.5 nm. Since the Au-Au distance was 0.255 nm, the 1.4 nm stretching breadth indicates the formation of an atomic chain. Due to the effective interaction between Ce@C₈₂ and Au, the Au atomic chain was highly stabilized in the presence of Ce@C₈₂ molecules,²³ while long atomic chains were not

TABLE I. Summary of the conductance for the single C₆₀ and Ce@C₈₂ molecular junctions.

System	Conductance
Au/Ce@C ₈₂ /Au	–
Ag/Ce@C ₈₂ /Ag	$0.28 (\pm 0.05)G_0$
Au/C ₆₀ /Au	$0.3(\pm 0.1) G_0$
Ag/C ₆₀ /Ag	$0.5(\pm 0.1)G_0$

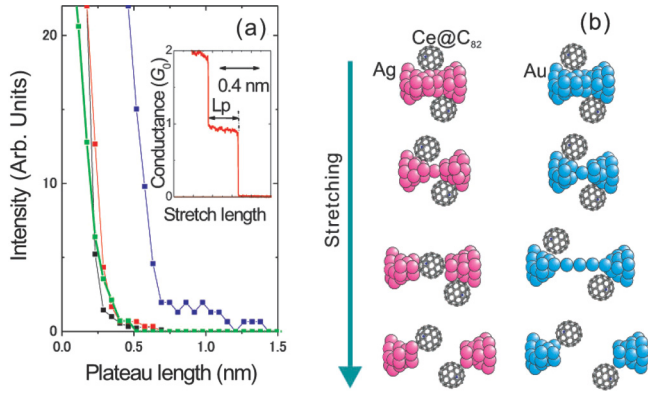


FIG. 3. (Color online) (a) Length histogram of the $1G_0$ plateau (L_p) for the Au and Ag contacts at the bias voltage of 100 mV. The blue, red, green, black curves are the results of the Au/Ce@C₈₂/Au, Ag/Ce@C₈₂/Ag, Au/C₆₀/Au junction, and clean Au contacts, respectively. The inset shows the typical conductance trace of the Au contacts before the introduction of Ce@C₈₂ at the bias voltage of 0.1 V. The intensity of the length histograms was normalized with the number of the conductance traces. The length histograms were constructed without data selection from 1000 conductance traces of breaking metal contacts. (b) Schematic view of the breaking process of the Au and Ag contacts. While the single molecular junction was formed for the Ag contact, the single molecular junction was not formed for the Au contact due to the large nanogap.

formed for the clean Au and Au in the presence of C₆₀ at 300 K. After breaking the Au atomic chain, the nanogap was formed between the Au electrodes. The gap size was sum of the length of the Au atomic wire (<0.5 nm) and contraction of the electrode (~0.5 nm).²⁴ The single Ce@C₈₂ molecule

could not be trapped in the Au nanogap due to its large gap size (~1.0 nm) as shown in Fig. 3.

III. AB INITIO CALCULATION

We have carried out first-principle calculations for the single C₆₀ and Ce@C₈₂ molecule junctions in order to shed light on the experimental observations of the single molecule junctions. The structure for free Ce@C₈₂ was optimized using the density functional theory (DFT) using the B3LYP functional^{25,26} and the SDD basis (with the SDD effective core potential) for Ce atom, and 3-21G, 6-31G*, 6-31 + G*, or 6-311G* basis for C atom as implemented in the GAUSSIAN program package.²⁷ The variation of the structure with the basis set on C was small and the optimized free structure was used as starting geometry in the following conductance calculations. The ground-state structure of Ce@C₈₂ has a C_{2v} symmetry, and the Ce atom is located at an off-cage-center position adjacent to a hexagonal ring along the C₂ axis of the cage with the average distance from the ring carbons of 2.534 Å at the B3LYP/6-311G*-SDD computational level. The B3LYP functional is the most commonly used DFT functional for fullerene calculations; if it is checked, for example, at the M06-2X/6-311G*-SDD level,²⁵ the shortest Ce-C contact has a similar value of 2.524 Å. In the optimized free Ce@C₈₂ structure more than two electrons are moved from the metal to the cage (measured by the Mulliken atomic charges, though the charge transfer depends on the calculational treatment and charge definition²⁷). Transport property calculations was performed using the nonequilibrium Green's function (NEGF) formalism and density functional theory (DFT) as implemented in the ATK 2008.10 code.^{28,29}

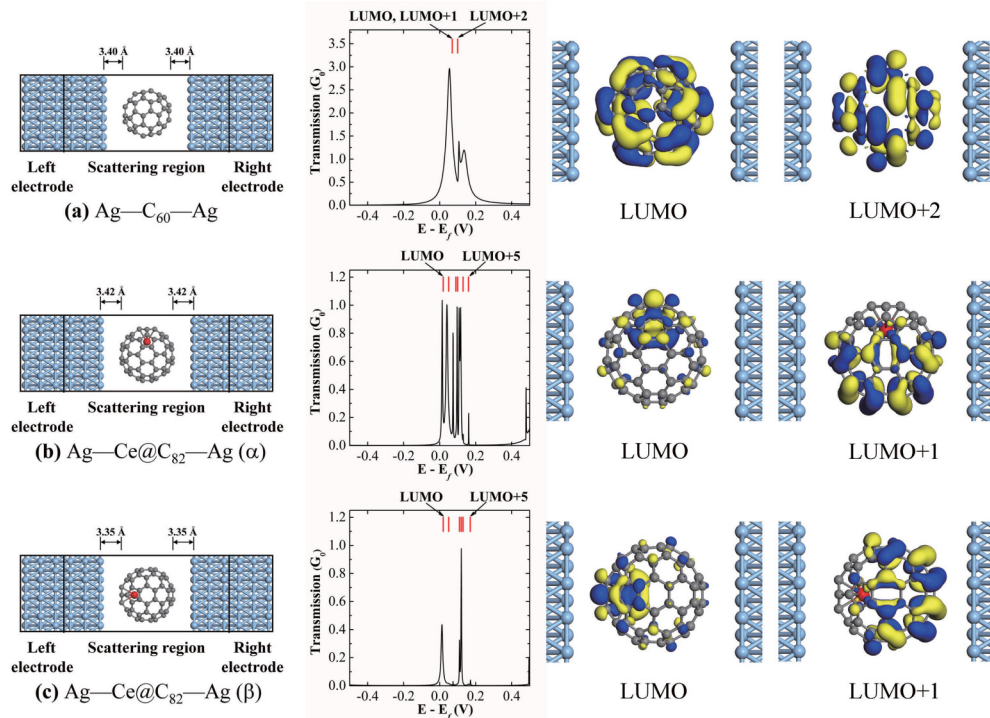


FIG. 4. (Color online) Structure models, transmission spectra (black) and MPSH energy spectra (red), and isosurfaces of the MPSH orbitals at zero bias voltage for the systems of (a) Ag/C₆₀/Ag, (b) Ag/Ce@C₈₂/Ag(α), (c) Ag/Ce@C₈₂/Ag(β). Red ball: Ce; blue ball: Ag; gray ball: C.

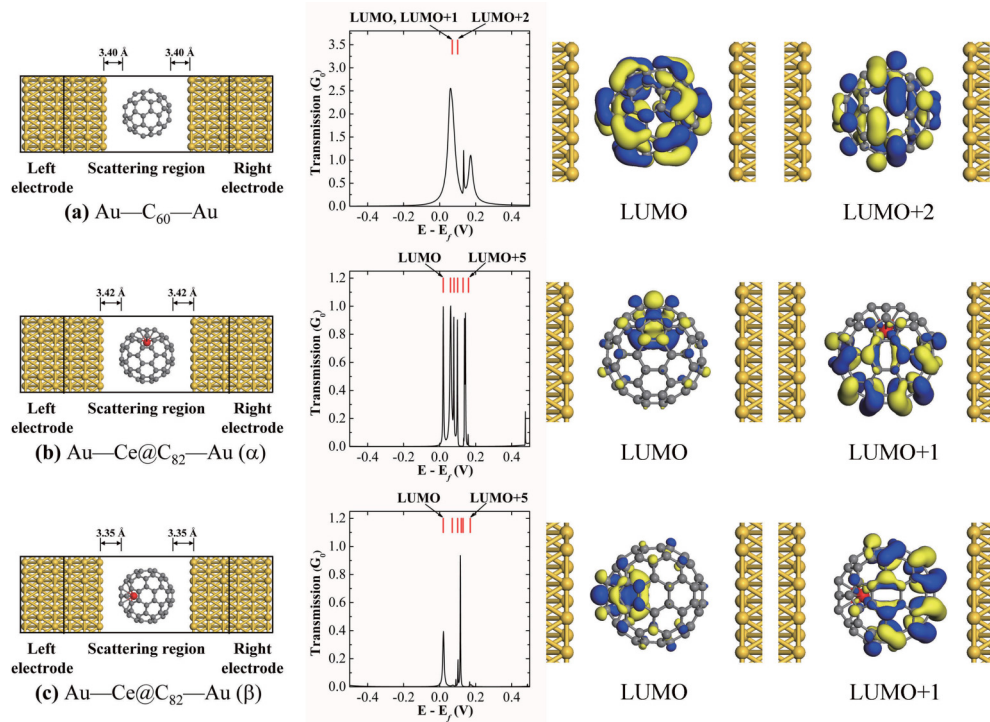


FIG. 5. (Color online) Structure models, transmission spectra (black) and MPSH energy spectra (red), and isosurfaces of the MPSH orbitals at zero bias voltage for the systems of (a) Au/C₆₀/Au, (b) Au/Ce@C₈₂/Au(α), (c) Au/Ce@C₈₂/Au(β). Red ball: Ce; yellow ball: Au; gray ball: C.

We employed a single- ζ basis set plus polarization with a mesh cutoff energy of 300 Ry, norm-conserving pseudopotentials, and a local density approximation (LDA).

We adopted a two-probe model where either a C₆₀ or Ce@C₈₂ molecule was sandwiched between semi-infinite gold (Fig. 5) or silver (Fig. 4) electrodes with a (111) surface cross-section. Hexagonal $5 \times 5 \times 3$ unit cells of $14.40 \times 14.40 \times 7.06 \text{ \AA}^3$ and $14.45 \times 14.45 \times 7.08 \text{ \AA}^3$ containing 75 atoms are used for Au and Ag electrodes, respectively. The k points of the electrodes are set to Monkhorst-Pack $1 \times 1 \times 50$. The structures are optimized until the maximum atomic force is less than 0.03 eV/\AA . Energy criterion of $1 \times 10^{-5} \text{ eV}$ was used in all the self-consistent calculations. The conductance of the single molecule junction depends on the atomic configuration of the metal electrodes.^{1,2} In the present study we investigated the (111) surface of Au and Ag electrodes. Although the absolute conductance value depends on the geometry of the surface, the relative conductance value is not sensitive to the geometry of the surface, when we compare the conductances of the single molecule junctions with the same geometry of the surface.³⁰ Hence, our results obtained from (111) surface of Au and Ag electrodes should be robust with respect to the geometry of the surface. Two configurations of Ce@C₈₂ were considered between electrodes. In configuration α [Fig. 4(b)] the C₂ axis of Ce@C₈₂ is parallel to the surfaces of the electrodes, whereas in configuration β [Fig. 4(c)] the Ce@C₈₂ molecule is rotated 90 deg so that the C₂ axis is perpendicular to the electrode surfaces. The distance between the molecule and the nearest metallic atoms was determined by optimizing the geometry of the molecule on top of the corresponding metallic surface. The relative position of the Ce atom in the carbon cage was also optimized.

We calculated the binding energies of junctions as $E_b = (E_s + E_m) - E_{S+M}$, where E_{S+M} , E_s , and E_m are the total energies for the electrode-slabs plus molecule, for only the electrode slabs, and for the isolated molecule, respectively. The distance between the molecule and the nearest metallic atoms was determined by optimizing the molecule on top of the corresponding metallic surface. The calculated binding energies of the Au/C₆₀/Au, Au/Ce@C₈₂/Au (α), Au/Ce@C₈₂/Au (β), Ag/C₆₀/Ag, Ag/Ce@C₈₂/Ag (α), and Ag/Ce@C₈₂/Ag (β) are 1.20, 1.28, and 1.31 eV, 1.14, 1.26, and 1.23 eV, respectively. These values were much larger than the physisorption energy. The weak chemical bond would be formed between Ce@C₈₂ and Au or Ag electrodes.

The electronic properties of electrodes were calculated with periodic conditions using the DFT scheme, and the Green's function as well as the self-energy of the central scattering region were obtained using the standard NEGF method. The electric current I under bias voltage V_{bias} was finally calculated using the Landauer-Büttiker formula:³¹

$$I(V_{\text{bias}}) = \frac{2e}{h} \int_{-\infty}^{\infty} \{T(E, V_{\text{bias}})[f_L(E - \mu_L) - f_R(E - \mu_R)]\} dE \quad (1)$$

where $T(E, V_{\text{bias}})$ is the transmission probability at a given bias voltage V_{bias} , $f_{L/R}$ is the Fermi-Dirac distribution function for the left (L)/right (R) electrode, and μ_L/μ_R is the electrochemical potential of the L/R electrode. The molecular-projected self-consistent Hamiltonian (MPSH) energy spectra and the corresponding MPSH orbitals were also calculated to illustrate the mechanism of the electron transport. The calculated conductances for the Au/C₆₀/Au

and Ag/C₆₀/Ag junctions are 0.506 and 0.790G₀, respectively, comparable with the corresponding experimental values of 0.3(±0.1) and 0.5(±0.1)G₀. The calculated conductance of the Au/Ce@C₈₂/Au (α), Au/Ce@C₈₂/Au (β), Ag/Ce@C₈₂/Ag (α), and Ag/Ce@C₈₂/Ag (β) are 0.159, 0.048, 0.212, 0.063G₀, respectively. The Mulliken population analysis revealed that there are 1.11, 1.12, 1.10, and 1.12 electrons transferred from Ce atom to carbon cage in the Ag/Ce@C₈₂/Ag(α), Ag/Ce@C₈₂/Ag(β), Au/Ce@C₈₂/Au(α), and Au/Ce@C₈₂/Au(β) configurations, respectively. The conductance histogram of the Ag/Ce@C₈₂/Ag junction showed a single peak at 0.28G₀, indicating the formation of one stable atomic configuration. The comparison between calculation and experimental results suggests that the Ag/Ce@C₈₂/Ag (α) junction would be preferentially formed under current experimental conditions. Both the experiments and calculations indicate that the conductance of the Ag/Ce@C₈₂/Ag junction was smaller than that of the Ag/C₆₀/Ag junction. The measured and calculated conductance of the former was smaller than that of the later by 44%³² and 73%, respectively.

Figure 4 shows the transmission spectra and MPSH energy spectra of Ag/C₆₀/Ag and Ag/Ce@C₈₂/Ag. The corresponding results of Au/C₆₀/Au and Au/Ce@C₈₂/Au are shown in Fig. 5. The electron transmissions are mainly contributed by MPSH states above the Fermi level (E_f), which are LUMO – LUMO + 2 for C₆₀ systems and LUMO – LUMO + 5 for Ce@C₈₂ systems. The small energy difference between LUMO – LUMO + 5 for Ce@C₈₂ and the Fermi level could relate with the conductance enhancement around ±0.12 V observed for Ag/Ce@C₈₂/Ag (see Fig. 2). The transmission coefficients of the major peaks in C₆₀ systems are about 2.5 times larger than those of the Ce@C₈₂ systems. Meanwhile, the transmission peaks are also much wider in C₆₀ systems than those of the Ce@C₈₂ ones. The transmission coefficients above E_f when C₆₀ was used as opposed to Ce@C₈₂ are attributed to the fact that the electrons are significantly more delocalized in C₆₀ than those in Ce@C₈₂. As showed in Figs. 4 and 5, the LUMO and LUMO + 1 MPSH of Ce@C₈₂ are more localized than those of C₆₀ most probably because of the interactions between the Ce atoms located at an off-center position,

and the carbon atoms around. This is why the conductance of C₆₀ systems was several times larger than that of systems involving Ce@C₈₂. Also, after the rotation of the Ce@C₈₂ from configuration α to configuration β was performed, we found that the MPSH states contribute less to the connection between the electrodes and, consequently, induce smaller conductances in configuration β .

IV. CONCLUSION

We have investigated single Ce@C₈₂ molecule bridging between metal electrodes. Single Ce@C₈₂ molecule junctions were fabricated using a MCBJ at 300 K under UHV. The electric conductance of the single Ce@C₈₂ molecule bridging between Ag electrodes was 0.28(±0.05)G₀. We were able to fabricate a single metallofullerene molecule junction showing a high and fixed conductance value via the direct binding technique. The conductance of the single Ce@C₈₂ molecule was smaller than that of the single C₆₀ molecule bridging between Ag electrodes, which was supported by theoretical calculations. The localization of electron in the Ce@C₈₂ molecule explained the reduction of the conductance of the single Ce@C₈₂ molecule junction. While the single Ce@C₈₂ molecule junction was formed for the Ag electrodes, it was not formed for the Au electrodes. The Ce@C₈₂ molecule could not be trapped in the large nanogap, which was formed after breaking the Au electrodes.

ACKNOWLEDGMENTS

This work was supported in part by a Grant-in-Aid for Scientific Research in Innovation Areas (No. 20108001), a Grant-in-Aid for Scientific Research (A) (No. 20245006), the Next Generation Super Computing Project (Nanoscience Project), Nanotechnology Support Project, Grants-in Aid for Scientific Research in Priority Areas (Nos. 20036008, 20038007) and Specially Promoted Research from the Ministry of Education, Culture, Sports, Science, and Technology of Japan, and the NSFC (Grant No. 10774003) and National 973 Projects (Grant No. 2007CB936200, MOST of China).

¹J. C. Cuevas and E. Scheer, *Molecular Electronics* (World Scientific, Singapore, 2010); N. Agrait, A. L. Yeyati, and J. M. van Ruitenbeek, *Phys. Rep.* **377**, 81 (2003).

²F. Chen, X. Li, J. Hihath, Z. Huang, and N. Tao, *J. Am. Chem. Soc.* **128**, 15874 (2006).

³Y. S. Park, A. C. Whalley, M. Kamenetska, M. L. Steigerwald, M. S. Hybertsen, C. Nuckolls, and L. Venkataraman, *J. Am. Chem. Soc.* **129**, 15768 (2007).

⁴L. Venkataraman, J. E. Klare, I. W. Tam, C. Nuckolls, M. S. Hybertsen, and M. L. Steigerwald, *Nano. Lett.* **6**, 458 (2006).

⁵A. Mishchenko, L. A. Zotti, D. Vonlanthen, M. Bürkle, F. Pauly, J. C. Cuevas, M. Mayor, and T. Wandlowski, *J. Am. Chem. Soc.* **133**, 184 (2011).

⁶W. Haiss, C. Wang, I. Grace, A. S. Batsanov, D. J. Schiffrin, S. J. Higgins, M. R. Bryce, C. J. Lambert, and R. J. Nichols, *Nat. Mater.* **5**, 995 (2006).

⁷J. M. Seminario, C. E. De La Cruz, and P. A. Derosa, *J. Am. Chem. Soc.* **123**, 5616 (2001).

⁸M. Kiguchi, O. Tal, S. Wohlthat, F. Pauly, M. Krieger, D. Djukic, J. C. Cuevas, and J. M. van Ruitenbeek, *Phys. Rev. Lett.* **101**, 046801 (2008).

⁹M. Kiguchi, T. Takahashi, T. Takahashi, T. Yamaguchi, T. Murase, M. Fujita, T. Tada, and S. Watanabe, *Angew. Chem., Int. Ed.* **50**, 5708 (2011).

¹⁰T. Bohler, A. Edtbauer, and E. Scheer, *Phys. Rev. B* **76**, 125432 (2007).

¹¹C. A. Martin, D. Ding, J. K. Sørensen, T. Bjørnholm, J. M. van Ruitenbeek, and H. S. J. van der Zant, *J. Am. Chem. Soc.* **130**, 13198 (2008).

¹²M. Kiguchi, *Appl. Phys. Lett.* **95**, 073301 (2009); M. Kiguchi and K. Murakoshi, *J. Phys. Chem. C* **112**, 8140 (2008).

- ¹³S. Nagase, K. Kobayashi, and T. Akasaka, *Bull. Chem. Soc. Jpn.* **69**, 2131 (1996).
- ¹⁴T. Wakahara, J. Kobayashi, M. Yamada, Y. Maeda, T. Tsuchiya, M. Okamura, T. Akasaka, M. Waelchli, K. Kobayashi, S. Nagase, T. Kato, M. Kako, K. Yamamoto, and K. M. Kadish, *J. Am. Chem. Soc.* **126**, 4883 (2004).
- ¹⁵L. Senapati, J. Schrier, and K. B. Whaley, *Nano Lett.* **4**, 2073 (2004).
- ¹⁶Y. Yasutake, Z. Shi, T. Okazaki, H. Shinohara, and Y. Majima, *Nano Lett.* **5**, 1057 (2005).
- ¹⁷J. Jiang, B. Gao, Z. P. Hu, W. Lu, Z. Y. Wu, J. L. Yang, and Y. Luo, *Appl. Phys. Lett.* **96**, 253110 (2010).
- ¹⁸A. J. Pérez-Jiménez, *J. Phys. Chem. C* **111**, 17640 (2007).
- ¹⁹A. Stróżecka, K. Muthukumar, A. Dybek, T. J. Dennis, J. A. Larsson, J. Mysliveček, and B. Voigtländer, *Appl. Phys. Lett.* **95**, 133118 (2009).
- ²⁰E. H. Huisman, C. M. Guédon, B. J. van Wees, and S. Jan van der Molen, *Nano Lett.* **9**, 3909 (2009); S. Guo, J. Hihath, I. Díez-Perez, and N. Tao, *J. Am. Chem. Soc.* **133**, 19189 (2011).
- ²¹M. A. Reed, C. Zhou, C. J. Muller, T. P. Burgin, and J. M. Tour, *Science* **278**, 252 (1997).
- ²²P. Reddy, S.-Y. Jang, R. A. Segalman, and A. Majumdar, *Science* **315**, 1568 (2007).
- ²³The adsorbed molecule decreased the surface energy of the Au atomic chain, which lead to the stabilization of the Au atomic chain. Improved stability of the metal atomic chain by adsorbed molecules was also observed for the Au contacts. H. X. He, C. Shu, C. Z. Li, and N. J. Tao, *J. Electroanal. Chem.* **522**, 26 (2002).
- ²⁴J. Zhao, K. Murakoshi, X. Yin, M. Kiguchi, Y. Guo, N. Wang, S. Liang, and H. Liu, *J. Phys. Chem. C* **112**, 20088 (2008).
- ²⁵A. D. Becke, *Phys. Rev. A* **38**, 3098 (1988); *J. Chem. Phys.* **98**, 5648 (1993); C. Lee, W. Yang, and R. G. Parr, *Phys. Rev. B* **37**, 785 (1988); X. Y. Cao and M. Dolg, *J. Mol. Struct., Theochem* **581**, 139 (2002); R. Krishnan, J. S. Binkley, R. Seeger, and J. A. Pople, *J. Chem. Phys.* **72**, 650 (1988); Y. Zhao and D. G. Truhlar, *Acc. Chem. Res.* **41**, 157 (2008).
- ²⁶M. J. Frisch *et al.*, Gaussian 09, Revision A.02, Gaussian, Inc., Wallingford CT, 2009.
- ²⁷V. Zólyomi, J. Koltai, J. Kürti, and S. Pekker, *Phys. Rev. B* **78**, 115405 (2008).
- ²⁸J. Taylor, H. Guo, and J. Wang, *Phys. Rev. B* **63**, 245407 (2001).
- ²⁹M. Brandbyge, J. L. Mozos, P. Ordejón, J. Taylor, and K. Stokbro, *Phys. Rev. B* **65**, 165401 (2002).
- ³⁰Z. Li and D. S. Kosov, *Phys. Rev. B* **76**, 035415 (2007).
- ³¹S. Datta, *Electronic Transport in Mesoscopic Systems* (Cambridge University Press, Cambridge, 1995).
- ³²The conductance of the single fullerene molecule junction depends on the atomic configuration of the junction. The discrepancy of the conductance of experimental results and theoretical calculation results can be explained by the other factors (e.g., atomic configuration of the electrodes) which was not considered in the theoretical calculation.